

# Self-Sealing Shells: Blowouts and Blisters on the Surfaces of Leaky Wind-Blown-Bubbles and Supernova Remnants

J.M. Pittard

*School of Physics and Astronomy, The University of Leeds, Leeds, LS2 9JT*

Accepted 2013 August 15. Received 2013 August 13; in original form 2013 July 9

## ABSTRACT

Blowouts can occur when a dense shell confining hot, high pressure, gas ruptures. The venting gas inflates a blister on the surface of the shell. Here we examine the growth of such blisters on the surfaces of wind-blown-bubbles (WBBs) and supernova remnants (SNRs) due to shell rupture caused by the Vishniac instability. On WBBs the maximum relative size of the blister ( $R_{\text{bstall}}/R$ ) is found to grow linearly with time, but in many cases the blister radius will not exceed 20 per cent of the bubble radius. Thus blowouts initiated by the Vishniac instability are unlikely to have a major effect on the global dynamics and properties of the bubble. The relative size of blisters on SNRs is even smaller than on WBBs, with blisters only growing to a radius comparable to the thickness of the cold shell of SNRs. The small size of the SNR blowouts is, however, in good agreement with observations of blisters in the Vela SNR. The difference in relative size between WBB and SNR blisters is due to the much higher speed at which gas vents out of WBBs, which translates into a greater energy flux through a rupture of a given size from interior gas of a given pressure. Larger blisters are possible if shell ruptures are bigger than expected.

We expect the observed velocity structure of SNR shells to be affected by the presence of blisters until the shell is no longer susceptible to ruptures, since the initial expansion of blisters is faster than the ongoing expansion of the shell.

**Key words:** hydrodynamics – shock waves – stars: mass loss – ISM: bubbles – stars: winds, outflows – (ISM:) supernova remnants

## 1 INTRODUCTION

The supersonic injection of material by stellar winds and/or supernovae into the surrounding environment leads to the formation of wind-blown bubbles (WBBs) and supernova remnants (SNRs). The gas swept up by these structures usually cools to form a dense shell which may be prone to the Vishniac (Vishniac 1983) overstability. This instability can grow from a linear perturbation and is characterised by an oscillation of the shock front and a power-law growth rate.

If the shell ruptures, hot, rarefied gas should flow at high speed into the undisturbed environment. In a study of the Vela SNR, Meaburn, Dyson & Hartquist (1988) concluded that such ruptures were responsible for inflating “blisters” on the surface of the swept-up shell. Since the gas swept-up by a blister also cools and forms a shell, the shell effectively “self-seals”. In the frame of reference of the main shell the blister will expand to a certain radius, stall, and then merge back into the shell. Meaburn et al. (1988) claim that the blisters that they detect are of comparable size to the thickness of the shell. The Vishniac instability has also been suggested to be responsible for the filamentary structure seen in

older SNRs (see Mac Low & Norman 1993, and references therein) and in the Eastern part of the WBB NGC 6888 (García-Segura et al. 1996).

In this work we study blisters on the surfaces of both WBBs and SNRs. Though the necessary conditions for shell rupture are not well known, we can nevertheless estimate the size of a resulting blister should a shell rupture occur. First we derive an expression for the evolution of the blister radius and determine the size of the blister at the time that it stalls. We then determine how the maximum size of a blister scales with the age of the underlying bubble or remnant, and we determine the maximum size of the blister relative to the original bubble/remnant. We discuss our analytical results for leaky WBBs in relation to numerical simulations where the Vishniac instability has been noted. We also compare our analytical results for leaky SNRs with observational data of remnants.

## 2 ANALYTICAL MODEL

### 2.1 General Considerations

The thickness of a cold WBB or SNR shell can be determined from mass conservation to be

$$\delta R = \frac{R}{5M^2}, \quad (1)$$

where  $M$  is the *adiabatic* Mach number of the shell into the surrounding medium and  $R$  is its radius<sup>1</sup>.

For expansion into a uniform environment the shell is continually decelerating and so is stable against Rayleigh-Taylor (RT) instabilities. However, the shell can be unstable to the Vishniac instability. In such cases, the shell is most unstable for perturbations with a wavenumber  $k$  where  $k\delta R \sim 1$ . This corresponds to a wavelength  $\lambda = 2\pi/k \sim 2\pi\delta R$  and a spherical harmonic mode number  $l = kR$ . The growth timescale for the instability is

$$\delta t_{\text{vish}} = \left( \frac{\sigma}{Pk^2|\ddot{R}|} \right)^{1/4}, \quad (2)$$

where  $\sigma$  is the surface density of the shell ( $\sigma = R\rho_0/3$ ),  $P$  is the interior thermal pressure of the hot gas and  $|\ddot{R}|$  is the effective deceleration of the shell. If the instability ruptures the shell it will create a gap through which the hot pressurized gas in the bubble/remnant interior can vent. The area of the “nozzle”  $A \approx \pi\lambda^2/4 \approx \pi^3\delta R^2$ . We assume that the size of the nozzle is constant in time, though in reality  $A$  is likely to increase due to the continued expansion of the main bubble/remnant and due to the ablation/stripping of material from its sides by the hot gas flowing through it. As well as widening the nozzle, this latter process would “mass-load” the interior of the blister.

The rate of energy release from the bubble or remnant interior into the “blowout” is given by the flux of kinetic and thermal energy through the nozzle,

$$\dot{E}_v = \left[ \frac{1}{2}\rho v^3 + \frac{Pv}{\gamma-1} \right] A, \quad (3)$$

where  $\rho$  is the interior density of the hot gas and  $v$  is the flow speed through the nozzle. The flow through such a nozzle will be transonic so we set  $v = c$  where  $c$  is the sound speed of the interior hot gas.

The vented material flows supersonically into the undisturbed ambient medium, and sweeps it up, so that a blister is formed on the surface of the bubble/remnant. The blister is bounded by a cold shell once its age exceeds the cooling time of the swept-up gas. The blister initially expands relatively rapidly, but like the main bubble/remnant it slows as it sweeps up more and more material. We assume that the blister “stalls” once its expansion velocity drops below that of the main bubble/remnant. While the blister is relatively modest in size (e.g.  $R_b \lesssim 0.1R$  where  $R_b$  is the blister radius), its shape is close to hemi-spherical. If it stalls while this condition is true its evolution follows that of a standard pressure-driven bubble (e.g. Dyson & Williams 1980), but with a slightly different constant of proportionality:

<sup>1</sup> This is equivalent to  $\delta R = \frac{R}{3M_{\text{iso}}^2}$  where  $M_{\text{iso}}$  is the *isothermal* Mach number of the shell.

$$R_b = \left( \frac{125}{77\pi} \right)^{1/5} \left( \frac{\dot{E}_v}{\rho_0} \right)^{1/5} t_b^{3/5}. \quad (4)$$

Note that the rate of energy venting,  $\dot{E}_v$ , and the time since the blowout,  $t_b$ , replace the equivalent  $\dot{E}$  and  $t$  of a standard WBB.

The swept-up gas becomes thermally unstable and collapses into a thin shell when the cooling time becomes less than the age of the blister. Assuming a strong adiabatic shock, a cold shell forms at

$$\delta t_{\text{cb}} = (2.3 \times 10^4 \text{ yr}) n_0^{-0.71} \dot{E}_{v,38}^{0.29}, \quad (5)$$

where  $n_0$  is the number density of the ambient medium and  $\dot{E}_{v,38}$  is the vented energy flux in units of  $10^{38} \text{ erg s}^{-1}$  (Mac Low & McCray 1988). If the blister expands into ionized gas with  $\mu m_{\text{H}} \approx 10^{-24} \text{ g}$ ,

$$\delta t_{\text{cb}} = 9.9 \times 10^{-17} \rho_0^{-0.42} \dot{E}^{0.145} \dot{M}^{-0.145} c_0^{1.16} t^{0.58}, \quad (6)$$

where  $c_0$  is the adiabatic sound speed of the ambient medium and cgs units are used throughout.

The age of the blister when its expansion velocity drops below that of the main bubble/remnant is

$$\delta t_{\text{stall}} = \left( \frac{125}{77\pi} \right)^{1/2} \left( \frac{\dot{E}_v}{\rho_0} \right)^{1/2} \left( \frac{5\dot{R}}{3} \right)^{-5/2}. \quad (7)$$

At this time, the radius of the blister is

$$R_{\text{bstall}} = \left( \frac{125}{77\pi} \right)^{1/5} \left( \frac{\dot{E}_v}{\rho_0} \right)^{1/5} \delta t_{\text{stall}}^{3/5}, \quad (8)$$

and the ratio  $R_b/R$  is a maximum for this particular blister. After this time the blister begins to merge back into the main bubble/remnant as it is overtaken by material in the adjacent cold shell. Substituting Eq. 7 into Eq. 8 gives

$$R_{\text{bstall}} = \left( \frac{125}{77\pi} \right)^{1/2} \left( \frac{\dot{E}_v}{\rho_0} \right)^{1/2} \left( \frac{5\dot{R}}{3} \right)^{-3/2}. \quad (9)$$

We assume that the main WBB/SNR shell is susceptible to the Vishniac instability until its Mach number declines to the point where the shell becomes too thick for the instability to grow. This occurs at  $t = t_{\text{nr}}$  when the density jump at the shell corresponds to an effective ratio of specific heats of  $\gtrsim 1.1$  for WBBs (Ryu & Vishniac 1988) and  $\gtrsim 1.2$  for SNRs (Ryu & Vishniac 1987; Vishniac & Ryu 1989).

### 2.2 Wind-Blown Bubble Specifics

Mass and energy injection by a star or group of stars is often observed to inflate a bubble in the surrounding medium. The swept-up gas becomes thermally unstable and collapses into a thin shell when the cooling time becomes less than the age of the bubble. The radius of a pressure-driven bubble with a thin swept-up shell is (e.g. Dyson & Williams 1980)

$$R = \left( \frac{125}{154\pi} \right)^{1/5} \left( \frac{\dot{E}}{\rho_0} \right)^{1/5} t^{3/5}, \quad (10)$$

where  $\dot{E}$  is the rate of energy injection into the bubble by stellar winds and/or supernovae,  $\rho_0$  is the mass density of the ambient medium, and  $t$  is the age of the bubble.

The thermal pressure within the bubble is given by

$$P = \rho_0 \dot{R}^2 + \frac{1}{3} \rho_0 \ddot{R}R, \quad (11)$$

where  $\dot{R}$  and  $\ddot{R}$  are the expansion speed and acceleration of the bubble, respectively (Dyson & Williams 1980). Substituting for  $\dot{R}$  and  $\ddot{R}$  one obtains

$$P = \frac{7}{(3850\pi)^{2/5}} \dot{E}^{2/5} \rho_0^{3/5} t^{-4/5}. \quad (12)$$

The average density within the bubble is

$$\rho \approx \frac{3\dot{M}t}{4\pi R^3}, \quad (13)$$

where  $\dot{M}$  is the rate of mass injection into the bubble by stellar winds and/or supernovae and we have ignored the volume occupied by the freely streaming wind in the bubble centre. We have also assumed that there is no evaporation of mass from the swept-up shell into the bubble interior (Weaver et al. 1977), or mass-loading from the destruction of clouds overrun by the shell (e.g. Pittard et al. 2001a,b). The interior sound speed of the bubble is  $c = (\gamma P/\rho)^{1/2}$ . Substituting this, the equation for  $A$ , and Eqs. 12 and 13 into Eq. 3 gives, for  $\gamma = 5/3$ ,

$$\dot{E}_v = 8.74 \rho_0^{3/2} R^{5/2} \dot{M}^{-1/2} c_0 t^{1/2}. \quad (14)$$

Since  $R \propto t^{3/5}$ , we find that  $\dot{E}_v \propto t^2$ .

Substituting Eq. 14 into Eq. 9, and replacing  $\dot{R}$  with  $3R/5t$ , yields

$$R_{\text{bstop}} = 2.27 \rho_0^{3/10} \dot{M}^{-1/4} c_0^2 \dot{E}^{-1/20} t^{8/5}. \quad (15)$$

Since the radius of the main bubble increases as  $t^{3/5}$ , we see that the maximum relative size of a blister ( $R_{\text{bstop}}/R$ ) increases linearly with the bubble age,  $t$ .

Since  $\delta R = R/(5M^2)$  and  $M = \dot{R}/c_0 = 3R/(5c_0t)$ , the thickness of the swept-up shell increases with time as

$$\delta R = 0.728 c_0^2 \left(\frac{\dot{E}}{\rho_0}\right)^{-1/5} t^{7/5}. \quad (16)$$

Hence the relative thickness of the shell is

$$\frac{\delta R}{R} = 0.955 c_0^2 \left(\frac{\dot{E}}{\rho_0}\right)^{-2/5} t^{4/5}. \quad (17)$$

Combining Eqs. 15 and 16 gives the ratio of the maximum size of a blister to the shell thickness as

$$\frac{R_{\text{bstop}}}{\delta R} = 3.12 \rho_0^{1/10} \dot{M}^{-1/4} \dot{E}^{3/20} t^{1/5}. \quad (18)$$

As noted in Sec. 2.1, rupturing of the shell by the Vishniac instability stops when the density jump at the shell corresponds to an effective ratio of specific heats of  $\gtrsim 1.1$ . The density jump at an adiabatic shock with  $\gamma \approx 1.1$  is  $\approx (\gamma + 1)/(\gamma - 1) \approx 21$ . An isothermal shock produces an equivalent density jump for an isothermal Mach number  $M_{\text{iso}} \approx \sqrt{21}$ . For a  $\gamma = 5/3$  gas this corresponds to an adiabatic Mach number  $M = M_{\text{iso}}/\sqrt{\gamma} \approx 3.55$ . Thus we assume that shell ruptures stop when the shell Mach number drops below 3.55. This corresponds to a time of

$$t_{\text{nr}} \approx 0.169 \frac{R}{c_0} \approx 5.965 \times 10^{-3} c_0^{-5/2} \left(\frac{\dot{E}}{\rho_0}\right)^{1/2}. \quad (19)$$

Substituting into Eq. 15 gives the maximum possible size of any blister (which occurs when  $t = t_{\text{nr}}$ ) as

$$R_{\text{bmax}} = 6.3 \times 10^{-4} \rho_0^{-1/2} \dot{M}^{-1/4} c_0^{-2} \dot{E}^{3/4}. \quad (20)$$

The radius of the main bubble at this time is

$$R = 0.0353 \left(\frac{\dot{E}}{\rho_0}\right)^{1/2} c_0^{-3/2}. \quad (21)$$

Hence, the maximum relative size of the blister is

$$\frac{R_{\text{bmax}}}{R} = 1.8 \times 10^{-2} \left(\frac{\dot{E}}{\dot{M}}\right)^{1/4} c_0^{-1/2}. \quad (22)$$

Writing  $\dot{E} = 0.5\dot{M}v_{\text{wind}}^2$ , we finally obtain

$$\frac{R_{\text{bmax}}}{R} = 1.5 \times 10^{-2} \left(\frac{v_{\text{wind}}}{c_0}\right)^{1/2}. \quad (23)$$

At  $t = t_{\text{nr}}$  it also follows that

$$\delta R \approx 5.6 \times 10^{-4} c_0^{-3/2} \left(\frac{\dot{E}}{\rho_0}\right)^{1/2}, \quad (24)$$

and

$$\frac{R_{\text{bmax}}}{\delta R} = 1.126 c_0^{-1/2} \left(\frac{\dot{E}}{\dot{M}}\right)^{1/4} = 0.947 \left(\frac{v_{\text{wind}}}{c_0}\right)^{1/2}. \quad (25)$$

### 2.3 Supernova Remnant Specifics

Supernova explosions drive high Mach number shocks into the surrounding interstellar medium (ISM). The shock-heated gas forms a SNR which initially expands freely, but which slows as the mass it sweeps up becomes comparable to and then exceeds the ejecta mass. The swept-up mass is concentrated in a thick shell behind the forward shock and the whole remnant is hot ( $T \gtrsim 10^7$  K) and expands adiabatically in what is known as its Sedov-Taylor (ST) stage (Taylor 1950; Sedov 1959). Eventually the expansion speed of the SNR becomes low enough that the post-shock gas begins to lose significant energy through radiative cooling. The thick shell becomes compressed into a thin dense shell of cooled gas which continues to be driven forward by the high pressure, hot and low-density interior in what is known as the pressure-driven snowplough (PDS) stage (McKee & Ostriker 1977). It is at this time that the Vishniac instability may play an important role.

The key input parameters for our model are the initial mechanical energy of the supernova explosion,  $E_0$ , and the density and temperature of the ambient medium,  $\rho_0$  and  $T_0$  respectively, which we assume are uniform.

The transition of the SNR to the radiative phase has been studied in detail by a number of works including Blondin et al. (1998). Assuming a strong shock, and an ionized medium with cosmic abundances, the cooling time of gas immediately behind the forward shock of the SNR is equal to the age of the remnant at the transition time

$$t_{\text{tr}} \approx (2.9 \times 10^4 \text{ yr}) n_{\text{H0}}^{-9/17} E_{51}^{4/17}, \quad (26)$$

where  $n_{\text{H0}}$  is the number density of hydrogen in the ambient medium and  $E_{51} = E_0/(10^{51} \text{ ergs})$ . The radius and velocity of the remnant at this time are respectively

$$R_{\text{tr}} \approx (19.1 \text{ pc}) n_{\text{H0}}^{-7/17} E_{51}^{5/17} \quad (27)$$

and

$$\dot{R}_{\text{tr}} \approx (260 \text{ km s}^{-1}) n_{\text{H0}}^{2/17} E_{51}^{1/17}. \quad (28)$$

Blondin et al. (1998) note that the actual time of shell formation, as determined from hydrodynamical calculations, is

$t_{\text{sf}} \approx 1.6 \times t_{\text{tr}}$ . The value of  $t_{\text{sf}}/t_{\text{tr}}$  is sensitive to the ambient density, increasing from 1.32 when  $n_{\text{H0}} = 8400 \text{ cm}^{-3}$  to 1.85 for  $n_{\text{H0}} = 0.084 \text{ cm}^{-3}$ .

To calculate the growth timescale of the Vishniac instability we need to know the rate of deceleration of the shell. The radius of remnants is often described in terms of a power-law with respect to time:  $R \propto t^m$ . During the ST stage  $R_{\text{ST}} \propto t^{2/5}$ , while in the pressure-driven snowplough stage  $R_{\text{PDS}} \propto t^{2/7}$ . However, simulations show that there is not a smooth transition between the ST and PDS stages and that in practice thin shell formation in SNRs often generates secondary shocks (e.g., Falle 1981). These cause the forward shock and the deceleration parameter,  $m = d(\log R)/d(\log t)$ , to undergo strong oscillations for a period of time after formation of the cold shell. Numerical studies show that after these oscillations have damped out  $m$  increases to a maximum value of 0.33 (e.g., Blondin et al. 1998), before converging asymptotically to the pressure-driven snowplough value of  $2/7$  (McKee & Ostriker 1977; Bandiera & Petruk 2004).

To avoid having to conduct full numerical simulations of this process we make use of the simple functional fit to  $m$  presented by Bandiera & Petruk (2004). For the slow branch (the physically relevant case) the deceleration parameter

$$m_{\text{s}}(r) = \frac{2}{35} \frac{r-1}{r^4} (5r^3 + 6r^2 + 8r + 16) + \frac{\sqrt{r-1}}{r^4} C, \quad (29)$$

where  $C = -0.248 \pm 0.006$  and  $r = 1.176 R/R_{\text{tr}}$ . Bandiera & Petruk (2004) also provide an expression for  $\tau = t/\tilde{t}$  as a function of  $r$ :

$$\tau_{\text{s}}(r) = \frac{2}{35} \sqrt{r-1} (5r^3 + 6r^2 + 8r + 16) + C, \quad (30)$$

where  $\tilde{t} = 1.14 t_{\text{tr}}$ . Hence for a specified value of  $r$  we can obtain the age of the remnant  $t$  and also a value for the deceleration parameter,  $m$ . Since  $m = \dot{R}t/R$ , where  $\dot{R}$  is the expansion speed of the remnant, we can then determine the shell velocity and adiabatic Mach number,  $M$ . The deceleration rate of the shell is given by  $\ddot{R} = (m-1)\dot{R}/t$ .

For simplicity we assume that a thin shell has formed once  $t \gtrsim 1.6 t_{\text{tr}}$ , and that the mass swept-up by the remnant is fully contained within it. This should be a good approximation since the interior density of a SNR is very low<sup>2</sup>.

The pressure jump at the shock is given by the standard Mach-number dependent Rankine-Hugoniot condition:

$$P_{\text{s}} = \frac{2\gamma M^2 - (\gamma - 1)}{\gamma + 1} P_0. \quad (31)$$

where  $P_0$  is the pressure of the ambient medium.

The exact values to use for  $\rho$  and  $P$  in Eq. 3 are a little uncertain because the density and pressure of the gas inside the remnant varies with the distance from the centre of the remnant. For guidance we refer to the numerical results of Blondin et al. (1998) where they claim that only the outermost 5 per cent of the remnant structure is affected by radiative cooling<sup>3</sup>. We therefore make the approximation

that the properties of the flow through the nozzle are equivalent to the hot phase at a radius of  $\approx 0.93R$ . From Fig. 5 in Blondin et al. (1998) we then determine that  $\rho \approx 1.5 \rho_0$  and  $P \approx 0.3P_{\text{s}}$ . The sound speed of this gas then follows:  $c = \sqrt{\gamma P/\rho}$ .

If the cold shell expands at a sufficiently high Mach number, Eq. 31 can be approximated as

$$P_{\text{s}} \approx \frac{2\gamma M^2}{\gamma + 1} P_0, \quad (32)$$

and then

$$v \approx c \approx \sqrt{\frac{\gamma P}{\rho}} \approx \gamma \sqrt{\frac{2M^2}{5(\gamma + 1)} \frac{P_0}{\rho_0}}. \quad (33)$$

Eq. 3 then evaluates to

$$\dot{E}_{\text{v}} \approx 0.701 P_0^{3/2} \rho_0^{-1/2} R^2 M^{-1}. \quad (34)$$

Substituting Eq. 34 into Eq. 4 yields:

$$R_{\text{b}} \approx 0.7m^{-1/5} c_0^{4/5} R^{1/5} t_b^{3/5} t^{1/5}. \quad (35)$$

Since the remnant radius  $R = at^m$ , the radius of an individual blister increases with time as  $R_{\text{b}} \propto m^{-1/5} t^{(1+m)/5} t_b^{3/5}$  until it reaches its maximum radius (at  $t_{\text{b}} = \delta t_{\text{stall}}$ ):

$$R_{\text{bstall}} \approx 0.191 m^{-2} c_0^2 R^{-1} t^2. \quad (36)$$

Thus the maximum blister size as a function of the remnant age,  $t$ , grows as  $R_{\text{bstall}} \propto m^{-2} t^{2-2m}$ . The relative size of such blisters is

$$\frac{R_{\text{bstall}}}{R} \approx 0.191 \left( \frac{c_0}{ma} \right)^2 t^{2-2m}. \quad (37)$$

Since

$$\delta R = \frac{R}{5M^2} = \frac{1}{5R} \left( \frac{c_0 t}{m} \right)^2, \quad (38)$$

we further find that

$$\frac{R_{\text{bstall}}}{\delta R} \approx 0.954. \quad (39)$$

Hence individual blisters do not grow larger than the thickness of the shell! This is in stark contrast to the case of blisters formed by the shell ruptures of wind-blown-bubbles, which as we have seen in Sec. 2.2 can grow much larger than the shell thickness.

The Vishniac instability stops at  $t = t_{\text{nr}}$  once the cold shell becomes too thick, which as noted in Sec. 2.1 occurs when the density jump at the shell corresponds to an effective ratio of specific heats of  $\gtrsim 1.2$ . Using the same argument as in Sec. 2.2, we find that this corresponds to an adiabatic Mach number  $M \approx 2.57$  for SNRs i.e. when  $\dot{R} \approx 2.57 c_0$ . At this time  $m$  is near its maximum value of 0.33 (see Fig. 1 of Bandiera & Petruk 2004). Since  $\dot{R} = mR/t$ , and  $r = 1.176 R/r_{\text{tr}}$ , we find that

$$t_{\text{nr}} = m \frac{R}{\dot{R}} \approx \frac{0.33}{2.57} \frac{r}{c_0} \approx 0.128 \frac{R}{c_0}. \quad (40)$$

This compares to  $t_{\text{nr}} \approx 0.169 R/c_0$  for leaky wind-blown bubbles.

of shell formation, though a reverse shock develops and heats gas in this region after  $t = 2.0 - 2.5 t_{\text{tr}}$  (see Fig. 6 in Blondin et al. 1998).

<sup>2</sup> At the time of transition into the radiative phase  $\approx 50$  per cent of the interior mass is compressed into the thin shell. However, the mass in the thin shell approaches the swept up mass at later times (Chevalier 1974; Mansfield & Salpeter 1974).

<sup>3</sup> Note that the gas adjacent to the shell is also cool at the time

At  $t = t_{\text{nr}}$ ,  $\delta R/R \approx 1/33$  and  $P_s \approx 8P_0$ , so  $P = 12P_0/5$ . The velocity of gas through the nozzle is then  $v = \sqrt{8P_0/(3\rho_0)}$ . With  $A = \pi^3 \delta R^2$  we obtain

$$\dot{E}_v \approx 0.26 P_0^{3/2} \rho_0^{-1/2} R^2, \quad (41)$$

so that the maximum possible size of a blister on a remnant shell is

$$R_{\text{bmax}} = \left(\frac{125}{77\pi}\right)^{1/2} \left(\frac{3}{5}\right)^{3/2} \left(\frac{\dot{E}_v}{\rho_0}\right)^{1/2} \left(\dot{R}_{\text{nr}}\right)^{-3/2}, \quad (42)$$

where  $\dot{R}_{\text{nr}}$  is the expansion speed of the remnant at  $t = t_{\text{nr}}$ . Substituting Eq. 41 into Eq. 42 one obtains

$$\frac{R_{\text{bmax}}}{R} \approx 0.028. \quad (43)$$

This is an unexpected result and indicates that the maximum relative size of a blister on the surface of a SNR does not depend on the explosion energy, the ambient density or the ambient temperature. We again see that the maximum size of a blister is comparable to the shell thickness (since at  $t = t_{\text{nr}}$ ,  $\delta R \approx R/33$ ).

### 3 ANALYTICAL RESULTS

In this section we use the analytical model developed in the previous section to examine the key characteristics of blisters on the surfaces of WBBs and SNRs. To allow a like-for-like comparison we assume that the WBBs and SNRs expand into an ambient medium with  $\rho_0 = 10^{-24} \text{ g cm}^{-3}$  and  $T_0 = 10^4 \text{ K}$  unless otherwise noted. We assume that the mass fractions of hydrogen, helium and metals are  $X = 0.705$ ,  $Y = 0.275$  and  $Z = 0.020$ , respectively, which gives an average particle mass of  $0.615 m_{\text{H}}$  when the gas is fully ionized. The corresponding sound speed for these conditions is  $c_0 = 15 \text{ km s}^{-1}$ .

#### 3.1 WBB Results

We consider first the evolution of blowouts around a bubble with the following key parameters:  $\dot{M} = 10^{-6} M_{\odot} \text{ yr}^{-1}$ ,  $v_{\text{wind}} = 2000 \text{ km s}^{-1}$ ,  $\rho_0 = 10^{-24} \text{ g cm}^{-3}$ ,  $T_0 = 10^4 \text{ K}$  and  $c_0 = 15 \text{ km s}^{-1}$ . The rate of energy injection,  $\dot{E} = 1.26 \times 10^{36} \text{ erg s}^{-1}$ . The wind injection parameters are typical of a single massive star. We refer to this model as WBB-A.

Fig. 1 shows that the bubble radius in model WBB-A grows to over 100 pc by  $10^7 \text{ yr}$ . The thickness of the cold swept-up shell grows from  $\approx 3 \times 10^{-3} \text{ pc}$  at the point of its formation when the bubble age is 6565 yr, to 38 pc at  $5 \times 10^6 \text{ yr}$ . The increasing thickness of the cold shell is caused by the continual decline in its Mach number as more and more material is swept-up. The shell has a Mach number of 10 when the bubble is 5760 yr old, and a Mach number of 3.5 when it is 80,000 yr old. The shell becomes subsonic when the bubble is 1.82 Myr old. Vishniac instabilities grow very rapidly as soon as the shell is formed ( $\delta t_{\text{vish}}/t \approx 0.07$ ), and so the shell is likely to rupture soon afterwards. Blowouts will then occur and will quickly develop and form cold shells ( $\delta t_{\text{cb}}/t \approx 0.07$ ). Hence the main WBB shell is indeed “self-sealing”. Since  $\delta t_{\text{cb}}/t$  declines as the age of the WBB increases this is true at all times.

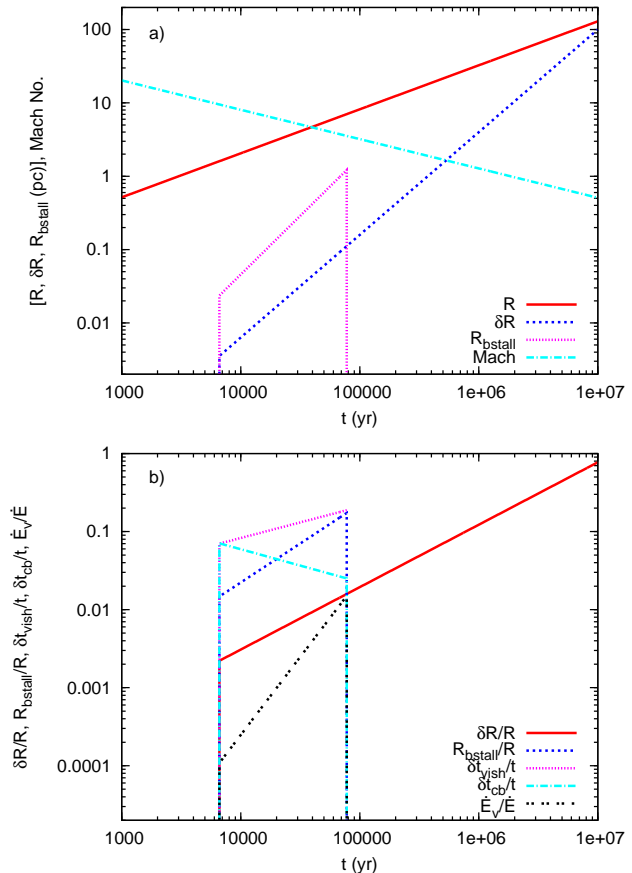


**Figure 1.** Top: The WBB radius ( $R$ ), Mach No. and shell thickness ( $\delta R$ ), and the blister radius at the point its expansion stalls ( $R_{\text{bstall}}$ ), as a function of time for model WBB-A. Bottom:  $\delta R/R$ ,  $R_{\text{bstall}}/R$ ,  $\delta t_{\text{vish}}/t$ ,  $\delta t_{\text{cb}}/t$  and  $\dot{E}_v/\dot{E}$  as a function of time for model WBB-A.

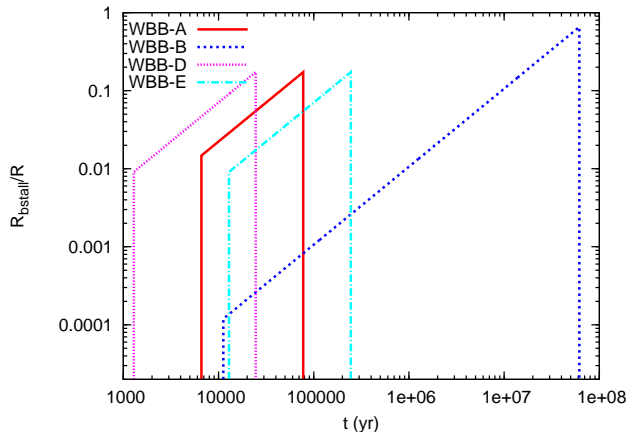
Blister created soon after cold shell formation of the main WBB are relatively small, however, because the rupture in the shell is also small. Thus the earliest blisters stall once they have reached a radius of 0.02 pc (this compares to a bubble radius of 1.6 pc at this time). However, blisters have the opportunity to become significantly larger as the shell slows and thickens, due to a corresponding increase in size of the ruptures and the “nozzle” which inflates them. Fig. 1 shows that blisters can reach a maximum radius of 1.22 pc at  $t = 0.078 \text{ Myr}$ . After this time, the Vishniac instability can no longer rupture the shell. Thus for model WBB-A, the maximum blowout radius  $R_{\text{bmax}} = 0.173 R$  (cf. Eq. 23). Each leakage event has an energy flux of at most  $0.015 \dot{E}$ .

The temperature of the hot gas within the main WBB is constant in time (at least while this gas remains adiabatic), so the flow speed of gas through ruptures is also independent of time. In model WBB-A, the temperature of the interior is  $\approx 4.5 \times 10^7 \text{ K}$ , and gas venting through a shell rupture has a velocity of  $\approx 1000 \text{ km s}^{-1}$ . The venting gas (which is transonic with respect to its own sound speed) has an adiabatic Mach number of 67 with respect to the surrounding medium. As we shall see, the gas venting from WBB ruptures is expelled at much higher speeds and temperatures than gas venting from SNR ruptures (cf. Sec. 3.2).

We have also investigated how the blisters depend on

**Table 1.** Assumed parameters for the WBB models and results. In all cases we assume  $v_{\text{wind}} = 2000 \text{ km s}^{-1}$ .

Model	$\dot{E}$ ( $\text{erg s}^{-1}$ )	$\rho_0$ ( $\text{g cm}^{-3}$ )	$T_0$ (K)	$c_0$ ( $\text{km s}^{-1}$ )	$t_c$ (yr)	$t_{\text{nr}}$ (yr)	$R_{\text{bmax}}$ (pc)	$R_{\text{bmax}}/R$
WBB-A	$1.26 \times 10^{36}$	$10^{-24}$	$10^4$	15	6600	$7.76 \times 10^5$	1.22	0.17
WBB-B	$1.26 \times 10^{36}$	$10^{-24}$	$10^2$	1.5	11200	$6.19 \times 10^7$	255	0.66
WBB-C	$1.26 \times 10^{36}$	$10^{-24}$	$10^7$	475	6600	13.8	-	-
WBB-D	$1.26 \times 10^{36}$	$10^{-23}$	$10^4$	15	1290	$2.45 \times 10^4$	0.38	0.17
WBB-E	$1.26 \times 10^{37}$	$10^{-24}$	$10^4$	15	12900	$2.45 \times 10^5$	3.84	0.17

**Figure 2.** The ratio of the radius of the stalled blister to the radius of the main WBB,  $R_{\text{bstall}}/R$ , as a function of time for some of the models noted in Table 1.

some key model parameters. Table 1 summarizes the different models that were analyzed. We have varied the energy injection rate,  $\dot{E}$ , and the ambient density and sound speed,  $\rho_0$  and  $c_0$ , respectively. The evolution of  $R_{\text{bstall}}/R$  for these models is shown in Fig. 2. Reducing the ambient sound speed (model WBB-B) results in a higher Mach number for the shell and consequently greater compression of the swept-up gas. This allows the shell to stay thinner for longer, extending the timescale over which the Vishniac instability may operate (up to a bubble age of  $t_{\text{nr}}$ ). This in turn increases the maximum value of  $R_{\text{bstall}}/R$  to 0.66, as confirmed using Eq. 23. However, to achieve this requires continuous energy input for nearly 62 million years. If the lifetime of the energy source is less than this (e.g., if the energy source is a single massive star), the value of  $R_{\text{bmax}}/R$  will be smaller.

In contrast, setting  $T_0 = 10^7 \text{ K}$  (model WBB-C) prevents any blowouts whatsoever. This is because the cold shell is already subsonic at its formation (at 6600 yr), and does not achieve the necessary compression for the Vishniac instability to operate<sup>4</sup>. This is also manifest by the fact that  $t_{\text{nr}} < t_c$ .

Increasing the ambient density (model WBB-D) causes the bubble evolution to speed up, but does not alter the maximum value of  $R_{\text{bstall}}/R$ . Indeed, Eq. 23 shows that there is no dependence on  $\rho_0$ . Increasing  $\dot{E}$  (model WBB-E) causes an increase in the bubble size, speed and Mach number at

any specified time. However, if  $\dot{M}$  is increased in proportion (i.e. so that a specific value of  $v_{\text{wind}}$  is maintained), we again see that the maximum value of  $R_{\text{bstall}}/R$  remains unaffected. Only by further reducing  $c_0$  or by increasing  $v_{\text{wind}}$  are we able to increase the maximum value of  $R_{\text{bstall}}/R$ . In reality, it may be difficult for a bubble to expand into a neutral or molecular medium if the central star has a high ionizing flux. One solution would be if the ionization front becomes trapped by the shell (e.g., Comerón 1997). In such a scenario the shell structure will be modified, and will consist of an inner ionized part and an outer neutral part. The Vishniac instability may then operate only in the outer neutral part of the shell. This is clearly beyond the scope of the present work.

### 3.2 SNR Results

We now consider the evolution of a SNR and the blowouts which may develop. We first adopt the following key input parameters:  $E_{51} = 1$ ,  $\rho_0 = 10^{-24} \text{ g cm}^{-3}$ ,  $T_0 = 10^4 \text{ K}$ . With these parameters,  $c_0 = 15 \text{ km s}^{-1}$ ,  $\mu_0 = 0.615$ , and  $n_{\text{H}0} = 0.97 \text{ cm}^{-3}$ . The remnant expands at its ST rate until cooling becomes important. We refer to this as model SNR-A - some key parameters are noted in Table 2.

Fig. 3a) shows that the remnant has formed a cool shell by an age of 50,000 yr (cf. Eq. 26). Just after this time the remnant has a radius of 22.4 pc, an expansion speed of  $114 \text{ km s}^{-1}$  and an adiabatic Mach number of 7.6. Note that the expansion speed and Mach number drop significantly during the process of cold shell formation as the remnant expansion stalls. The deceleration parameter,  $m$ , drops from 0.4 (just prior to cold shell formation the remnant expands according to the ST solution) to  $\approx 0.26$  (Fig. 3b). The cold shell is initially compressed quite thin ( $\delta R = 0.077 \text{ pc}$ ) and is subject to the Vishniac instability ( $\delta t_{\text{vish}} = 9590 \text{ yr}$ ).

Fig. 3c) shows that gas venting through a shell rupture at the time of cold shell formation has a temperature  $\approx 1.4 \times 10^5 \text{ K}$  and a velocity of  $57 \text{ km s}^{-1}$ . The venting gas has an adiabatic Mach number of 3.8 with respect to the surrounding medium. Hence it drives a shock into the undisturbed ISM and a blister rapidly develops. Such blisters reach their maximum size  $\approx 380 \text{ yr}$  after the shell rupture and take 750 yrs to form their own cold shells (and thus “self-seal” the remnant) - see the plots of  $\delta t_{\text{stall}}/t$  and  $t_{\text{cb}}/t$  in Fig. 3d), respectively. Note that blisters formed from shell ruptures at later times form cold shells prior to stalling. We note again that gas venting from WBB ruptures is expelled at much higher speeds and temperatures than gas venting from SNR ruptures (cf. Sec. 3.1). Note also that though

<sup>4</sup> Note that it is likely that we slightly underestimate the cooling time for cold shell formation since we assume a strong shock.

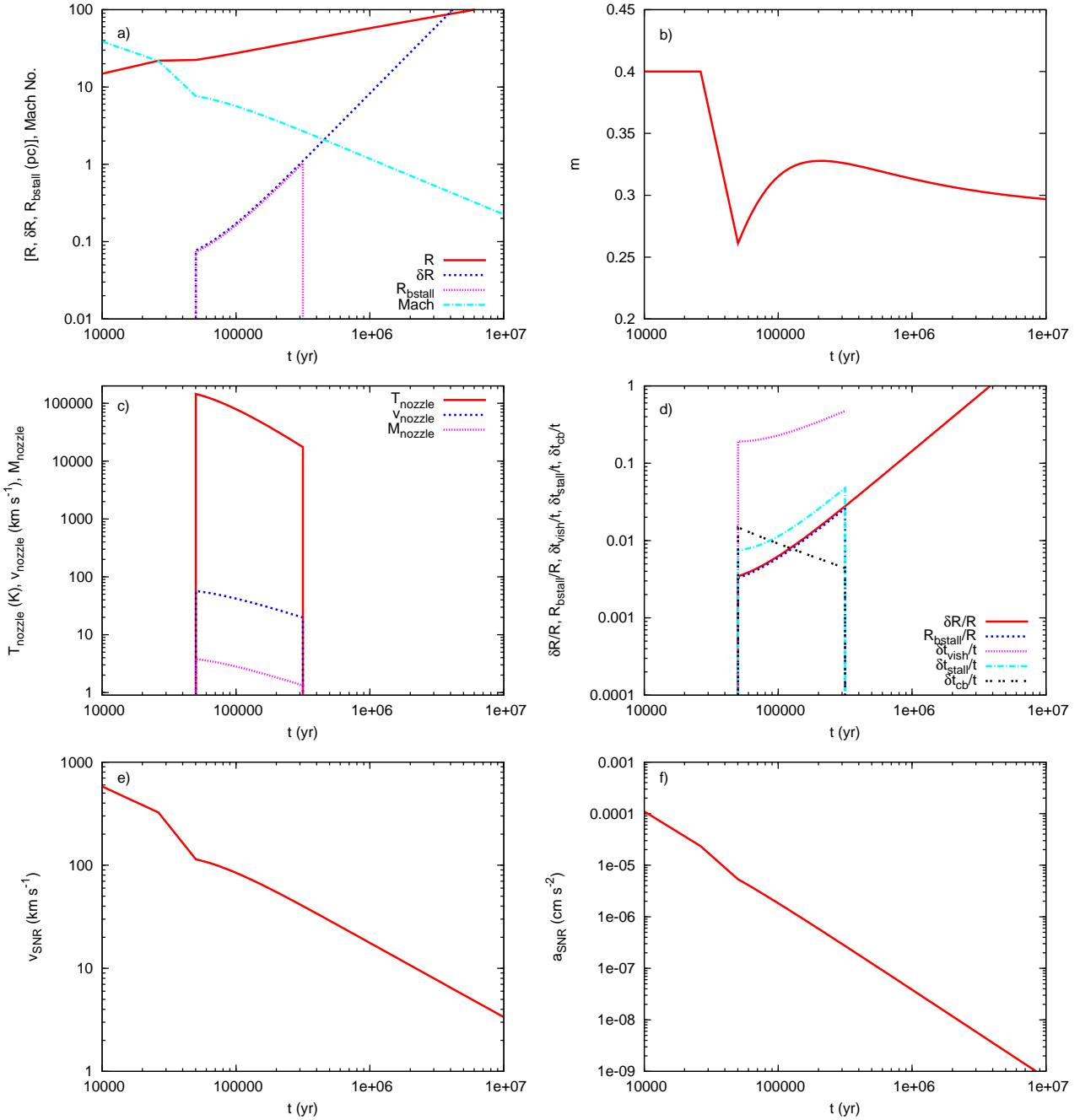


**Figure 3.** a) The SNR radius ( $R$ ), shell thickness ( $\delta R$ ) and maximum blowout radius ( $R_{\text{bstall}}$ ) as a function of time for model SNR-A. The adiabatic Mach number of the shell is also shown. b) The deceleration index,  $m$ , of the remnant vs. time. c) The temperature, velocity and Mach number (with respect to the ambient medium) of the flow through a rupture vs. time (the gas flow through the rupture is transonic). d)  $\delta R/R$ ,  $R_{\text{bstall}}/R$ ,  $\delta t_{\text{vish}}/t$ ,  $\delta t_{\text{stall}}/t$  and  $\delta t_{\text{cool,b}}/t$  as a function of time. e) The shell velocity vs. time. f) The shell deceleration rate vs. time.

$\dot{R} > v_{\text{nozzle}}$  for model SNR-A (cf. Figs. 3c and e), venting still occurs because the gas just interior to the shell is itself expanding at a speed very nearly equal to that of the shell.

Since  $\delta t_{\text{vish}}/t$  increases with time, the Vishniac instability is more likely to rupture the shell soon after formation of the cold shell. However, if ruptures continue to occur blisters grow to larger sizes before stalling as the remnant ages. At a time near the post-cold-shell peak in the deceleration parameter (which occurs at  $t \sim 0.2$  Myr), we measure from

Fig. 3a) that  $R_{\text{bstall}} \propto t^{1.64}$  (Eq. 36 gives  $R_{\text{bstall}} \propto t^{1.67}$  for  $m = 0.33$ ). This difference can be explained as due to the combination of the time dependence of  $m$  and our approximation of  $P_s$  in Eq. 32. The curvature in  $R_{\text{bstall}}/R$  reflects the time dependence of  $m$  (cf. Eq. 37).

Fig. 3a) shows that blisters can reach a maximum radius of 1.03 pc by  $t = t_{\text{nr}} = 0.316$  Myr, after which time the Vishniac instability can no longer rupture the shell (which has a radius  $R = 39.8$  pc). Thus for model SNR-A, the max-

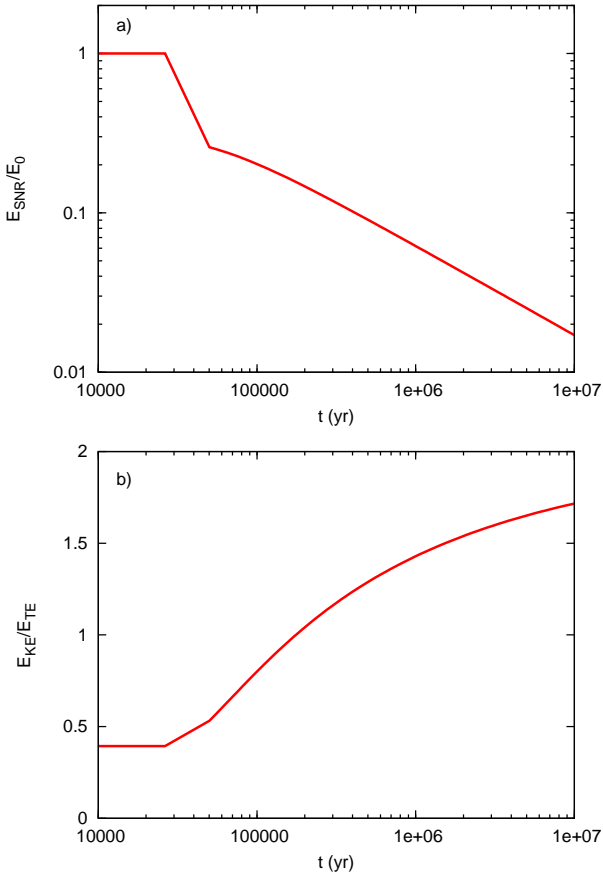


**Figure 4.** a) The energy of the remnant vs. time for model SNR-A. b) The ratio of the kinetic to thermal energy of the remnant vs. time.

imum blowout radius is  $\approx 0.026 R$  (cf. Eq. 43). Each leakage event involves an energy flux of at most  $5.9 \times 10^{33} \text{ erg s}^{-1}$ .

Bandiera & Petruk (2004) also provide equations for the ratio of the kinetic to thermal energy within the remnant (their Eq. 16) and for the total energy of the remnant (their Eq. 19). Note that the equations do not account for the thermal energy swept up by the remnant, which can be significant at late times. In Fig. 4a) we plot the ratio of the current energy of the remnant compared to its initial energy. The remnant radiates away 75 per cent of its energy during the process of cold shell formation (in good agreement with numerical simulations - see, e.g., Falle 1981; Pittard et al. 2003) and contains just 11 per cent of its energy at  $t = t_{\text{nr}}$ , 6 per cent at  $t = 1 \text{ Myr}$ , and only 5 per cent when the shell expansion becomes subsonic at  $t = 1.25 \text{ Myr}$ . During this interval the kinetic energy fraction of the remnant increases from 28 per cent to 60 per cent of the total remnant energy (Fig. 4b).

We have also investigated how the SNR blisters depend on some key model parameters. Table 2 summarizes the different models which were analyzed. We have varied the initial mechanical explosion energy,  $E_{51}$ , and the ambient density and sound speed,  $\rho_0$  and  $c_0$ , respectively. The evolution of  $R_{\text{bstall}}/R$  for these models is shown in Fig. 5a). Changing the values of  $E_{51}$  and  $\rho_0$  (compare models SNR-A to SNR-E) varies the rapidity of the remnant evolution and

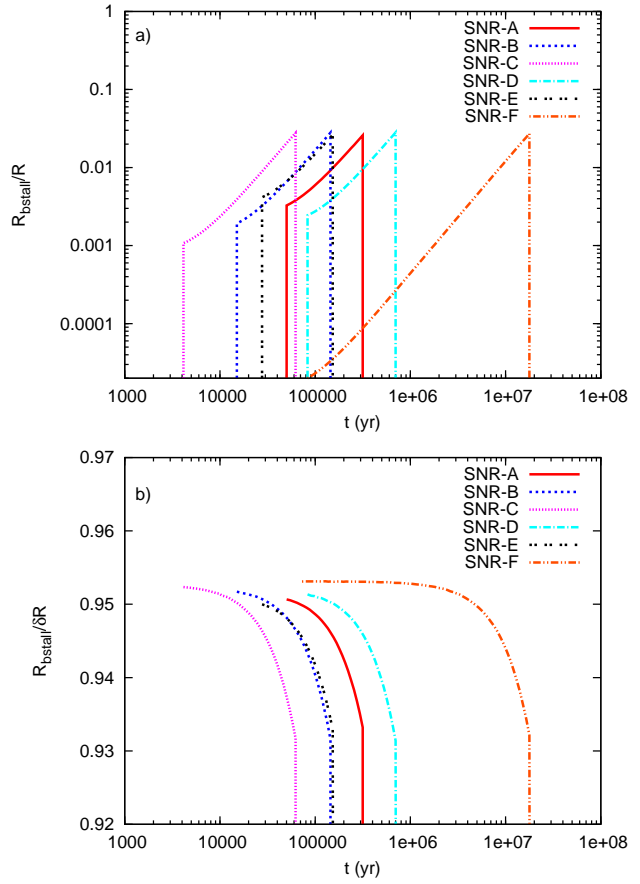


**Figure 5.** a) The ratio of the blister stall radius to the SNR radius ( $R_{\text{bstall}}/R$ ) as a function of time for some of the models noted in Table 2. b) The ratio of the blister stall radius to the shell thickness ( $R_{\text{bstall}}/\delta R$ ) as a function of time.

the Mach number of the shell at the time of cold shell formation. Therefore the stall radii of the blisters at the time of cold shell formation is different between these models. However, each model has the same maximum blowout radius relative to the remnant radius at  $t = t_{\text{nr}}$  ( $R_{\text{bmax}}/R$ ), which is expected given that Eq. 43 has no dependence on  $E_{51}$ ,  $\rho_0$  or  $c_0$ .

Remnants which expand into a cold medium are able to maintain supersonic shells for a considerably longer time interval (see model SNR-F). In contrast, remnants which expand into a very hot medium have shells with reduced Mach numbers. This can result in the Mach number of the cold shell at its formation being too low for the Vishniac instability to grow, thus preventing blowouts and blisters (model SNR-G).

Fig. 5b) shows the value of  $R_{\text{bstall}}/\delta R$  for our models. For shells at high Mach number the models show that  $R_{\text{bstall}}/\delta R \approx 0.95$  (cf. Eq. 39). The value of this ratio decreases as the Mach number of the shell drops and the thermal pressure becomes important in the shock jump conditions.



**Table 2.** Assumed parameters for the SNR models and results. Subscript *tr* indicates when the remnant transitions from adiabatic to radiative. A cool shell is assumed to form at  $t = 1.6 t_{\text{tr}}$  (see Sec. 2.3 for details). Subscript *nr* indicates when the cold shell becomes too thick for the Vishniac instability to continue to operate.  $M_{\text{su}}$  is the swept-up mass at  $t = t_{\text{tr}}$ . Model SNR-G forms a cold shell at a Mach number which is too low for the Vishniac instability to operate.

Model	$E_{51}$ ( $10^{51}$ ergs)	$\rho_0$ ( $\text{g cm}^{-3}$ )	$T_0$ (K)	$c_0$ ( $\text{km s}^{-1}$ )	$t_{\text{tr}}$ (yr)	$R_{\text{tr}}$ (pc)	$v_{\text{tr}}$ ( $\text{km s}^{-1}$ )	$\text{Mach}_{\text{tr}}$	$M_{\text{su}}$ ( $M_{\odot}$ )	$t_{\text{nr}}$ (yr)	$R_{\text{nr}}$ (pc)	$R_{\text{bmax}}$ (pc)	$R_{\text{bmax}}/R$
SNR-A	1	$10^{-24}$	$10^4$	15	29400	19.3	259	17.3	1006	$3.16 \times 10^5$	39.8	1.03	0.0259
SNR-B	1	$10^{-23}$	$10^4$	15	8700	7.49	340	22.7	586	$1.45 \times 10^5$	17.8	0.50	0.0280
SNR-C	1	$10^{-22}$	$10^4$	15	2570	2.90	445	29.8	341	$6.22 \times 10^4$	7.76	0.22	0.0278
SNR-D	10	$10^{-24}$	$10^4$	15	50600	38.0	297	19.8	7680	$7.00 \times 10^4$	85.1	2.40	0.0282
SNR-E	0.1	$10^{-24}$	$10^4$	15	17100	9.82	226	15.1	132	$1.53 \times 10^5$	19.1	0.50	0.0263
SNR-F	1	$10^{-24}$	$10^2$	1.5	43600	26.2	238	230	1200	$1.78 \times 10^7$	166	4.52	0.0273
SNR-G	1	$10^{-24}$	$10^7$	475	29400	19.3	259	0.55	1007	–	–	–	–

### 3.3 Comparison of WBB and SNR Results

We have seen from the work in the previous subsections that the relative size of blisters compared to their WBB or SNR host is greater for WBBs. We wish to understand why this is so. Fig. 6 compares various properties of models WBB-A and SNR-A. These models have the same ambient density  $\rho_0$ , temperature  $T_0$ , and sound speed  $c_0$ .

Fig. 6a) and b) show that the SNR model has a relatively larger shell radius during the period of interest when shell ruptures can occur, and that the velocity of the shell is also higher for the majority of this period too. We also see that the SNR model has a thicker cold shell than the WBB model at any given time after its formation (Fig. 6a). The pressure of the gas flowing through the shell rupture is roughly comparable during the period that shell ruptures occur in both models (roughly from 50,000 – 80,000 yr - see Fig. 6c). However, because shell ruptures start when the SNR is older the typical pressure of the flow through a rupture is less in the SNR model. More striking is the fact that the density of gas flowing through the rupture is much lower, and it flows out much more rapidly, in the WBB model (Figs. 6d and e). Finally, Fig. 6f) shows the relative size of blisters as a function of time for both models.

Eq. 3 gives the rate of energy venting through a shell rupture. With our assumption that the flow through the rupture is transonic ( $v = c$ ), we have

$$\dot{E}_v = \frac{7}{3} P c A \quad (44)$$

when  $\gamma = 5/3$ . With  $A \approx \pi^3 \delta R^2$  and  $\delta R = R/(5M^2)$ , we find using Eq. 9 that

$$\frac{R_{\text{bstall}}}{R} \approx 0.18 \left( \frac{Pc}{\rho_0} \right)^{1/2} c_0^2 \dot{R}^{-7/2}. \quad (45)$$

Since  $c = \sqrt{\gamma P/\rho}$ , this expression can also be written as

$$\frac{R_{\text{bstall}}}{R} \approx 0.21 P^{3/4} \rho^{-1/4} \rho_0^{-1/2} c_0^2 \dot{R}^{-7/2}. \quad (46)$$

Although the dependence on  $\rho$  is weakest out of all of these variables, it is the one whose value is most different between the two models. In the SNR model it is assumed to be constant with time and equal to  $1.5 \rho_0$ , whereas in the WBB model it is assumed to be equal to the average density of the hot interior gas (Eq. 13).

Table 3 notes values of interest from models WBB-A and SNR-A at the time of cold shell formation ( $t_c$ ) and at the time that the Vishniac instability ceases to operate ( $t_{\text{nr}}$ ). We see that the  $\dot{R}^{-7/2}$  term in Eqs. 45 and 46 favours (by about a factor of 2) a larger value of  $R_{\text{bstall}}/R$  for the SNR model. However, the  $(Pc)_{\text{nozzle}}^{1/2}$  term favours a larger value of  $R_{\text{bstall}}/R$  for the WBB model by a factor of 10 or more and so clearly dominates this comparison.

Both  $P$  and  $c$  contribute to the greater value of  $(Pc)_{\text{nozzle}}^{1/2}$  from the WBB model. However, inspection of the values for  $P$  and  $c$  in Table 3 reveals that it is the higher value of  $c$  which dominates. Hence, the greater relative size of blisters on WBBs is ultimately due to the much higher temperature of the hot interior gas in the WBB. This leads to a much faster flow through the rupture and consequently to a much higher energy flux through unit area of a rupture into the developing blister. Because the size of the rupture is related to the thickness and thus also to the radius of the shell, we see that the greater relative energy flux through a rupture in a WBB shell allows a larger blister to be blown for a given shell radius.

## 4 DISCUSSION

### 4.1 WBB Results

#### 4.1.1 Comparison to Numerical Simulations

In recent years there have been many published works on hydrodynamical simulations of WBBs. The Vishniac instability can be clearly identified in numerical simulations of a wind blowing into a uniform medium (e.g., Strickland & Stevens 1998; Dwarkadas 2001; Freyer et al. 2006), and in simulations which study the interaction of bubbles blown by massive stars (e.g., van Marle et al. 2012; Krause et al. 2013). In all of these works the swept-up shell is decelerating and is therefore stable to RT instabilities, which makes identifying the Vishniac instability quite straightforward. However, in situations where RT instabilities also occur (such as where a faster wind blows into a slower wind, e.g., García-Segura & Mac Low 1995; García-Segura et al. 1996; van Veelen et al. 2009; Toalá & Arthur 2011), identification of the Vishniac instability is less secure.

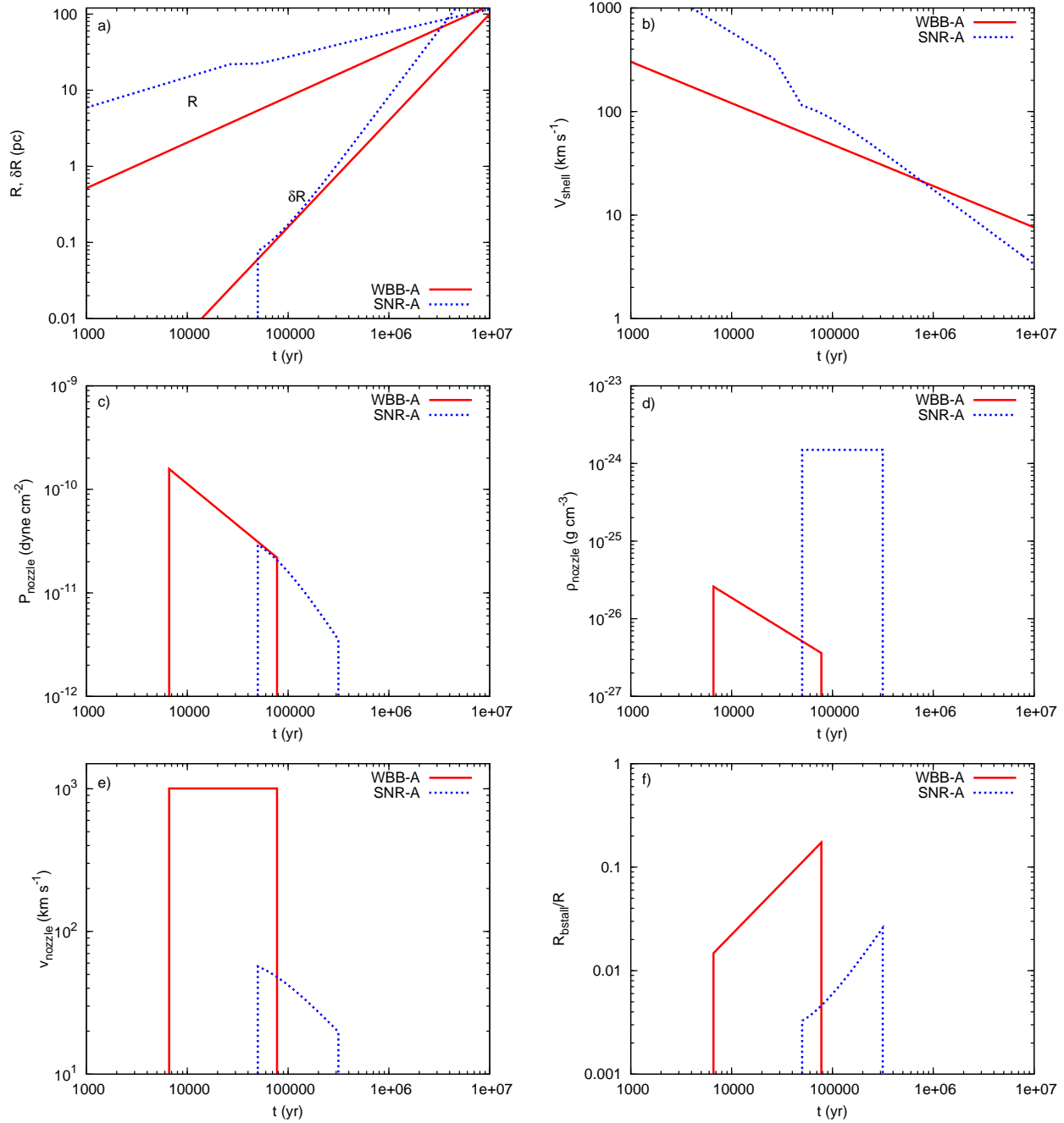


**Figure 6.** Comparison of models WBB-A and SNR-A. Shown as a function of time are a) the radius of the shell and its thickness; b) the shell expansion velocity; c-e) the pressure, density and velocity of gas as it flows through a shell rupture; f) the size of blisters relative to the radius of the main shell.

It is interesting that Dwarkadas (2007) notes that the Vishniac instability seen in his simulations was stronger in earlier models (e.g. Dwarkadas 2001). Since the latter were at lower resolution he expressed confusion at this finding. However, the assumed temperature of the ambient medium was different in the simulations ( $\sim 100$  K vs.  $\sim 8000$  K). We suggest that this difference is likely to be the underlying cause, since a lower ambient temperature keeps the Mach number of the shell higher, which results in a longer timescale over which the growth of the instabilities can op-

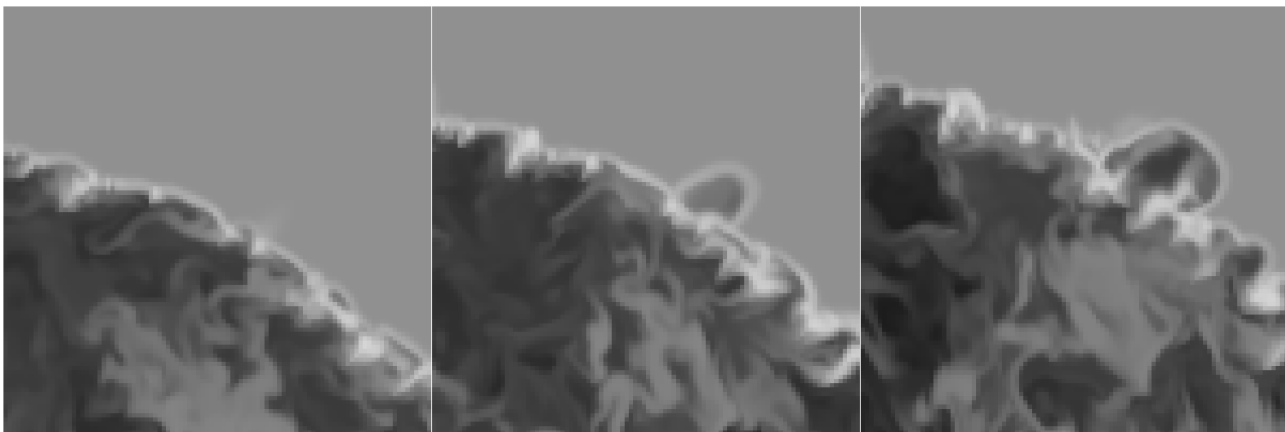
erate (and ultimately a greater relative blister radius cf. Eq. 23).

Table 4 summarizes work in the literature where Vishniac instabilities are noted in hydrodynamic simulations of WBBs. The main parameters adopted for the simulations are noted. We also note the time for cold shell formation,  $t_c \approx (2.3 \times 10^4 \text{ yr}) n_0^{-0.71} \dot{E}_{38}^{0.29}$ , and the time when the Vishniac instability ceases to operate,  $t_{\text{nr}}$  (Eq. 19). We can now study the published results in the light of these values.

Strickland & Stevens (1998) note that cooling of the swept-up gas and the process of shell formation takes several

**Table 3.** Comparison of the WBB and SNR parameters at given times. The ambient medium has identical properties in both models:  $\rho_0 = 10^{-24} \text{ g cm}^{-3}$ ,  $T_0 = 10^4 \text{ K}$  and  $c_0 = 15 \text{ km s}^{-1}$ . For model WBB-A,  $t_c = 6603 \text{ yr}$  and  $t_{\text{nr}} = 0.776 \text{ Myr}$ . For model SNR-A,  $t_c = 47,100 \text{ yr}$  ( $t_{\text{tr}} = 29,400 \text{ yr}$ ) and  $t_{\text{nr}} = 0.316 \text{ Myr}$ . Note that  $c_{\text{nozzle}}$  is less than the shell expansion velocity,  $\dot{R}$ , at all times in model SNR-A.

Model	t	R (pc)	$\dot{R}$ ( $\text{km s}^{-1}$ )	$P_{\text{nozzle}}$ ( $\text{dyn cm}^{-2}$ )	$\rho_{\text{nozzle}}$ ( $\text{g cm}^{-3}$ )	$T_{\text{nozzle}}$ (K)	$c_{\text{nozzle}}$ ( $\text{km s}^{-1}$ )	$M_{\text{nozzle}}$	$(Pc)_{\text{nozzle}}^{1/2}$ ( $\text{g}^{1/2} \text{s}^{-3/2}$ )	$R_{\text{bstall}}/R$
WBB-A	$t_c$	1.60	142	$1.57 \times 10^{-10}$	$2.6 \times 10^{-26}$	$4.52 \times 10^7$	1005	67	$4.0 \times 10^{-4}$	0.0147
	$t_{\text{nr}}$	7.03	53.1	$2.19 \times 10^{-11}$	$3.6 \times 10^{-27}$	$4.52 \times 10^7$	1005	67	$1.5 \times 10^{-4}$	0.173
SNR-A	$t_c$	22.4	114	$2.91 \times 10^{-11}$	$1.5 \times 10^{-24}$	$1.45 \times 10^5$	57	3.8	$4.1 \times 10^{-5}$	0.0033
	$t_{\text{nr}}$	39.8	40.2	$3.53 \times 10^{-12}$	$1.5 \times 10^{-24}$	$1.75 \times 10^4$	19.8	1.3	$8.4 \times 10^{-6}$	0.0259



**Figure 7.** Time series of blister growth from a 3D hydrodynamic simulation of a WBB. The blister can be seen growing from a rupture in the swept-up shell located near the centre of the left panel. The density scale is logarithmic between  $10^{-27} \text{ g cm}^{-3}$  (black) to  $10^{-19} \text{ g cm}^{-3}$  (white). The spatial scale of each panel is  $8 \times 8 \text{ pc}$ , and the size of each grid cell is  $0.0625 \text{ pc}$  (thus there are  $128 \times 128$  grid cells visible in each panel). The centre of the WBB is  $9.75 \text{ pc}$  below the bottom left corner of each panel. The time of each snapshot (left to right) is  $0.697 \text{ Myr}$ ,  $0.761 \text{ Myr}$  and  $0.823 \text{ Myr}$ . The simulation used the same setup as SimA from Rogers & Pittard (2013) but with the ambient density increased by a factor of 100. The large density variations within the bubble are extremely time-dependent and result from the ablation of dense gas closer to the stellar cluster.

1000 years, beginning at a bubble age of about 4000 years. This is in good agreement with the estimate of  $t_c$  in Table 4. While the Vishniac instability may operate up to a bubble age of about  $0.2 \text{ Myr}$  for the parameters adopted, the main focus of the Strickland & Stevens (1998) paper is not on the long-term evolution of the WBB, and the latest time at which a 2D plot of the density is shown is  $14630 \text{ yr}$  (see the bottom-right panel of their Fig. 1). The Vishniac instability is clearly seen at this time. We estimate that the relative scale of the shell perturbations,  $R_p = (R_{\text{max}} - R_{\text{min}})/\bar{R} \approx 0.04$ , where  $R_{\text{max}}$  ( $R_{\text{min}}$ ) is the maximum (minimum) radius of any part of the cold shell and  $\bar{R}$  is its average radius. The inferred value for  $R_p$  is larger than the expected size of blowouts at this time ( $R_{\text{bstall}}/R = 0.015$ ). We conclude, therefore, that the perturbations are not blowouts and that their larger than expected size results from under-resolving the shell: at  $t = 14630 \text{ yr}$  we expect a shell Mach number  $M = 9.6$ , a bubble radius  $R = 3.47 \text{ pc}$ , and a shell thickness  $\delta R = 0.0077 \text{ pc}$  (hence  $\delta R/R \approx 2 \times 10^{-3}$ ), whereas the size of the grid cells is  $0.0162 \text{ pc}$ .

The Vishniac instability is also seen in the simulations of Dwarkadas (2001), but unfortunately the information provided in this work is a little sparse. Nevertheless, using the values noted in Table 4 we estimate that shell formation

occurs at  $4200 \text{ yrs}$  and that the Vishniac instability could potentially operate until a bubble age of  $20 \text{ Myr}$ , aided by the lower sound speed of the ambient medium. Fig. 3 in Dwarkadas (2001) clearly shows Vishniac instabilities and there seems also to be evidence for shell ruptures and blisters. At  $t = 4.5 \text{ Myr}$  we estimate from his Fig. 3 that  $R_p \approx 0.09$ , though we predict that  $R_{\text{bstall}}/R = 0.18$  at this time.

Freyer et al. (2006) note that the Vishniac instability ceases early in the evolution of their simulated WBB (by  $t = 0.2 \text{ Myr}$ ), due to the increase in the shell thickness (note that the WBB expands into a medium with  $T \approx 8000 \text{ K}$  because of the presence of a HII region around their bubble). We estimate that  $t_c = 810 \text{ yr}$  and  $t_{\text{nr}} \approx 0.025 \text{ Myr}$ . Their Fig. 3 (at  $t = 700 \text{ yr}$ ) shows the existence of a shell but it is clear that at this stage it is too thick for rapid growth of the Vishniac instability, perhaps because the shell is still cooling and has yet to be fully compressed. However, the numerical resolution could also be a factor (there are only 32 cells per bubble radius and the shell thickness is about 5 cells). In contrast, their Fig. 4 (at  $t = 0.05 \text{ Myr}$ ) is already after the window of opportunity for the Vishniac instability. Despite these issues small perturbations are visible in both of their Figs. 3 and 4.

Ntormousi et al. (2011) investigate the interaction of the winds from several massive star clusters. Each cluster contains 50 stars with time-dependent mass and energy injection rates. During the first 3 Myr we estimate that each cluster has an average  $\dot{M} \approx 3 \times 10^{-5} M_{\odot} \text{ yr}^{-1}$  and  $\dot{E} \approx 7.7 \times 10^{37} \text{ erg s}^{-1}$  (and therefore an average  $v_{\text{wind}} \approx 2850 \text{ km s}^{-1}$ ). We determine that the Vishniac instability should occur up to a cluster age of about 0.79 Myr. Unfortunately the earliest plot of the density is at 3 Myr but the shell is clearly very unstable even at this time (see their Fig. 2). The authors note that 3 instabilities are simultaneously at work: Vishniac, thermal and Kelvin-Helmholtz. However, since the shocked gas can cool to a lower temperature than the pre-shock gas we believe that the behaviour of the shell is dominated by the thermal instability.

By far the best example of the Vishniac instability in numerical simulations of WBBs in the literature is in van Marle et al. (2012). Fig. 1 in this paper shows the main-sequence WBB around a  $40 M_{\odot}$  star at  $t = 4.3 \text{ Myr}$ . Vishniac instabilities are clearly seen (and expected) at this time. It is more difficult, even with the aid of the online movies, to decide whether the shell also ruptures and blisters form, but it is possible that this occurs in several places around the bubble. In any case we measure  $R_p \approx 0.18$ , in reasonable agreement with the predicted  $R_{\text{bstall}}/R = 0.30$  at this time. The numerical resolution is good, with about 250 cells per bubble radius at  $t = 4.3 \text{ Myr}$ .

Krause et al. (2013) investigate the collision of 3 WBBs. Their simulations are 3D and thus capture important new physics, but this means that they also suffer from poor resolution compared to some of the other 2D simulations described above. We estimate that up until  $t = 1.95 \text{ Myr}$ , the  $60 M_{\odot}$  star has an average mass-loss rate of  $\dot{M} \approx 3 \times 10^{-6} M_{\odot} \text{ yr}^{-1}$  and injects into the ISM an average energy flux of  $\dot{E} \approx 10^{37} \text{ erg s}^{-1}$  (hence an average  $v_{\text{wind}} \approx 3240 \text{ km s}^{-1}$ ). Using these values as input we find that the Vishniac instability could in theory occur up until a bubble age of  $\approx 30 \text{ Myr}$  (though a  $60 M_{\odot}$  star will not live this long). The shell perturbations seen around the WBB of the  $60 M_{\odot}$  star shown in the top right panel of their Fig. 3 at  $t = 1.95 \text{ Myr}$  have  $R_p \approx 0.25$ . This is nearly 5 times greater than the predicted value of  $R_{\text{bstall}}/R \approx 0.053$ . This discrepancy, like that of Strickland & Stevens (1998), may result from the low resolution (there are roughly 60 cells per bubble radius at this time, whereas we expect  $\delta R/R \approx 2 \times 10^{-3}$ ).

Finally we note that we have seen the Vishniac instability in our own simulations of WBBs and what we believe is the first unambiguous evidence for shell rupture and blowouts/blister formation. This behaviour was first reported by Rogers & Pittard (2013) and is shown here in Fig. 7. Although the (cluster) wind initially blows into a highly inhomogeneous medium, a roughly spherical bubble forms after this blows out into the surrounding uniform medium<sup>5</sup>. Fig. 7 focuses on a small part of the swept-up shell when the cluster wind has been blowing for 0.7 – 0.8 Myr.

<sup>5</sup> At these later stages the flow has some similarities to a standard WBB (e.g., there is a reverse shock which heats the wind to high temperatures while a forward shock sweeps up and compresses the ambient medium into a thin shell). However, the centre of the bubble contains a large reservoir of cold, dense gas which is slowly ablated by the cluster wind and mixed into the bubble interior,

The left-most panel shows the initial rupture of the swept-up shell (the shell has a width of  $\delta R = 2 - 3$  grid cells). The hot gas in the bubble interior then vents through this opening, blowing the blister which is seen expanding in the other two panels. At later times the identity of the blister is compromised by the growth of other nearby blisters. Unfortunately the nature of this simulation means that it is not possible to run the analysis in Sec. 2 on it. Note also that when the ambient temperature is 8000 K, the swept-up shell remains too thick for the Vishniac instability to efficiently operate and no blisters occur (cf. Fig. 1 in Rogers & Pittard 2013).

## 4.2 SNR Results

### 4.2.1 Numerical and Experimental Investigations of the Vishniac Instability

The growth of the Vishniac instability during the pressure-driven snowplough stage of a supernova remnant has been investigated numerically by Mac Low & Norman (1993), Blondin et al. (1998) and Michaut et al. (2012). Mac Low & Norman (1993) used a 2D spherical polar grid with  $128 \times 256 (r, \theta)$  zones to investigate the stability of adiabatic blast waves with various values of  $\gamma$ . They found that the Vishniac instability saturates for relatively small amplitudes, but can still produce density variations of more than a factor of two in the swept-up shell. They also note that there is only a finite time during which the cold SNR shell is unstable, because for a typical SNR evolving into a warm ionized ISM with  $n_0 < 1 \text{ cm}^{-3}$ , the Mach number after shell formation is  $< 5$  (while growth of perturbations requires  $M \gtrsim 2.6$ ). They find that the radial perturbation of the shell is always quite small ( $\Delta r/R \approx 0.02$ ). They do not observe any disruption or fragmentation of the shell, though if many eigenmodes were included in the initial perturbation this may have occurred. They claim that the instability is stronger in SNRs than in WBBs because of the more rapid deceleration of SNRs.

The Vishniac instability has also been investigated by Blondin et al. (1998) in their simulations of the radiative phase in SNRs. Using 2D simulations, with  $10^4 \times 250$  effective  $(r, \theta)$  zones and a realistic cooling function, they find that a 1 per cent perturbation (an  $l = 128$  spherical harmonic) of an average ISM density of  $n_{\text{H0}} = 0.84 \text{ cm}^{-3}$  leads to shell perturbations of similar size to the shell thickness. Increasing the average ISM density to  $n_{\text{H0}} = 84 \text{ cm}^{-3}$  causes the shell to break into a complicated structure of filaments that extend over the outer 10 per cent of the SNR radius. However, in this case the shell is very thin and the non-linear thin-shell instability (Vishniac 1994; Blondin & Marks 1996) dominates the (initial) behaviour.

Michaut et al. (2012) performed a numerical simulation of the Vishniac instability during the pressure-driven snowplough stage of a supernova remnant. They find that the initial growth of the instability is quickly damped as the remnant expands, the Mach number of the shell decreases, and the shell thickens. The remnant is observed to slow extremely rapidly as it expands into a high pressure

and which significantly affects the bubble structure, morphology and evolution (see also Pittard et al. 2001a,b).

**Table 4.** Summary of work where the Vishniac instability has been identified in hydrodynamic simulations of WBBs.  $n_{\text{amb}}$ ,  $T_{\text{amb}}$  and  $c_{\text{amb}}$  are the ambient number density, temperature and sound speed, respectively. Our calculations were computed using the value noted for  $c_{\text{amb}}$ . The paper references are as follows: SS98 = Strickland & Stevens (1998), D01 = Dwarkadas (2001), F06 = Freyer et al. (2006), N11 = Ntormousi et al. (2011), vM12 = van Marle et al. (2012), K13 = Krause et al. (2013).

Paper	$n_{\text{amb}}$ ( $\text{cm}^{-3}$ )	$T_{\text{amb}}$ (K)	$c_{\text{amb}}$ ( $\text{km s}^{-1}$ )	$\dot{M}$ ( $M_{\odot} \text{ yr}^{-1}$ )	$v_{\text{wind}}$ ( $\text{km s}^{-1}$ )	$\dot{E}$ ( $\text{ergs s}^{-1}$ )	$t_{\text{c}}$ (yr)	$t_{\text{nr}}$ (Myr)
SS98	10	$10^4$	15	$5 \times 10^{-5}$	2000	$6.3 \times 10^{37}$	4000	0.17
D01	$\sim 1$	$\sim 10^2$	1.5	$\sim 10^{-7}$	$\sim 3000$	$\approx 2.8 \times 10^{35}$	4200	20
F06	20	$8 \times 10^3$	13.4	$\sim 3 \times 10^{-7}$	$\sim 4000$	$1.5 \times 10^{36}$	810	0.025
N11	1	$8 \times 10^3$	13.4	← Cluster →			21300	0.79
vM12	20	$10^2$	1.5	$10^{-6}$	2000	$1.26 \times 10^{36}$	770	9.4
K13	10	121	1.65	← 3 winds + SNe →			2300	30

( $p/k \sim 10^7 \text{ K cm}^{-3}$ ), high temperature ( $T \sim 10^6 \text{ K}$ ) environment. It remains to be seen if a simulation with a lower ambient density and temperature will develop more vigorous Vishniac instabilities that might lead to the rupture of the shell.

Instabilities and radiative shocks have also been produced with lasers in high energy laboratory experiments (e.g. Edens et al. 2010, and references therein). However, the interpretation of the results is often difficult, and clear evidence of the Vishniac instability has yet to be presented.

#### 4.2.2 Observations of Blisters

The shells of SNRs in their PDS stage show complex filamentary morphologies and velocity fields. The filaments are likely caused by ripples in the shock front which are viewed at a range of angles (Hester 1987). The source of the ripples could be variations in the pre-shock gas, though it might also be caused by the Vishniac instability (see Mac Low & Norman 1993).

Shull (1983) reported turbulent motions in Vela’s shell with speeds up to  $30 \text{ km s}^{-1}$  and characteristic scales of deformation of  $\approx 0.01 \text{ pc}$ . Absorption datasets of the Vela SNR indicate that the velocity is chaotic with high observed line-of-sight velocities near the edges of the remnant as well as towards its centre (Jenkins, Wallerstein & Silk 1984; Danks & Sembach 1995). This is unexpected since an ellipse in velocity-spatial datasets is expected from coherent expansion of the shell, and indicates that some process is creating transverse motions.

To interpret the complicated ultra-violet absorption structure found by Jenkins et al. (1984), Meaburn et al. (1988) introduced the concept of blisters on the surface of the shell which form when the shell ruptures, and which self-seal due to the ablation of material from the main part of the shell. Echelle spectra of  $\text{H}\alpha$  and  $[\text{NII}]$  emission presented by Meaburn et al. (1988) revealed the presence of these blisters, which were found to have a maximum size comparable to the shell thickness. It is interesting to note that our analytical calculations are in agreement with this conclusion. Meaburn et al. (1990) and Greidanus & Strom (1992) present data of the SNRs IC 443 and the Cygnus Loop, respectively, which may also be consistent with the blister model. In Vela, the Cygnus Loop, and IC 443 radial velocity variations of order  $\pm 100 - 200 \text{ km s}^{-1}$  exist. Although this is somewhat higher than the expected flow

speed through the nozzle (see Fig. 3c), the gas will accelerate further as it blows out into the surrounding medium and such speeds may be achievable.

More recently, Gvaramadze (1998, 1999) interpret circular filaments on the face of the Vela SNR as due to the expanding shells of blisters. The characteristic size of the blisters is about  $1^\circ$ , which is a much larger scale relative to the size of the remnant than Eq. 43 predicts. To reconcile this discrepancy requires that the ruptures in the shell be larger than expected (since  $R_{\text{bmax}} \propto \dot{E}_{\text{v}}^{1/2}$  in Eq. 42, a rupture with  $10\times$  the radius increases  $\dot{E}_{\text{v}}$  by 2 dex and  $R_{\text{bmax}}$  by 1 dex). This is perhaps not beyond the bounds of possibility considering that the flow through the rupture should ablate the surrounding shell and thus act to widen the rupture. A detailed hydrodynamic study of this process would be useful.

Finally, we note that a series of more than 10 neighbouring loops together form the so-called Honeycomb nebula in the Large Magellanic Cloud (Wang 1992). The loops are of sizes  $2 - 3 \text{ pc}$ , and the object is interpreted as forming when a SN shock wave encounters an intervening sheet of dense, but porous, interstellar gas along our line of sight (Meaburn et al. 1995; Chu et al. 1995). The loops appear as collimated flows with velocity  $\sim 100 - 200 \text{ km s}^{-1}$  directed towards the observer (Meaburn et al. 1995). However, some of the cells show evidence for self-sealing blisters, which may occur when the magnetic pressure no longer dominates the gas pressure in the flow (Redman et al. 1999). Meaburn et al. (2010) claim that *Chandra* images are more indicative of emission from the centre of each cell rather than poorly resolved boundary layers. Since some cells also show red-shifted velocity spikes Meaburn et al. (2010) discuss the possibility of a young SNR in the edge of a giant shell. Again, a detailed hydrodynamic study of this object would be beneficial.

## 5 SUMMARY

This paper investigates the size of blisters resulting from breaks in the swept-up shell of a wind-blown bubble or a supernova remnant. The breaks are assumed to occur due to the Vishniac instability. We have developed a simple analytical model to describe the evolution of such blisters.

We find that blisters on the surfaces of WBBs are almost always small in scale relative to the size of the bubble ( $R_{\text{bstail}}/R \lesssim 0.2$ ), with this ratio increasing linearly with

time until the shell is thick enough to prevent any further ruptures. The maximum relative size of the blisters ( $R_{\text{bmax}}/R$ ) scales only as  $(v_{\text{wind}}/c_0)^{0.5}$  (cf. Eq. 23).

Since blowouts are confined and the blisters “self-seal” and tend to be relatively small, shell ruptures cannot be globally important to WBBs (e.g. they cannot be responsible for the lower than expected temperatures inside WBBs) except in the most extreme cases. It is clear, therefore, that truly “leaky bubbles” require density inhomogeneities in the surrounding medium (as envisaged by, e.g., Tenorio-Tagle et al. 2006; Harper-Clark & Murray 2009) and cannot occur in smooth media. We note, however, that even when shells run over density inhomogeneities, leakage is not guaranteed, since the shell can also re-seal behind it producing a long extended tail in the process (see Pittard 2011).

The relative size of blisters on SNRs is even smaller, with blisters resulting from breaks in the swept-up shell of a SNR in its PDS stage only growing to radii comparable to the thickness of the cold shell (Eq. 39), unless the blowout widens the rupture or the initial rupture is larger than expected. Unexpectedly we find that the maximum relative size of the blisters on SNRs does *not* depend on key parameters of the model, such as the initial mechanical energy of the explosion,  $E_0$ , or the density and temperature of the ambient ISM,  $n_{\text{H0}}$  and  $T_0$  respectively (see Eq. 43). The predicted size of the blisters and the velocity of the gas associated with them appear to be in rough accordance with observations of SNR shells.

Since the initial expansion of the blisters is faster than that of the main shell, blisters should affect the observed velocity structure of SNR shells while they exist. Thus SNR shells should only start to show a coherent velocity versus radius structure, instead of a messy velocity structure at all radii, once blisters can no longer form, which occurs when the shell’s Mach number has dropped low enough to shut off the Vishniac instability. Future hydrodynamical simulations of this process will be of interest.

The analytical model developed in Sec. 2 of course incorporates many simplifications. For instance, we have assumed that the WBB/SNR and the shell rupture are essentially static while the blister grows to its maximum size. We have also assumed that when a WBB expands into an ionized medium that the ionization front is not subsequently trapped by the swept-up shell. If this were to occur it would reduce the ambient sound speed,  $c_0$ , and thus increase the shell Mach number and the compression of newly swept-up gas. Ultimately this may allow the Vishniac instability to continue operating for a longer time in such scenarios, or allow it to (re-)start (since  $t_{\text{nr}}$  increases). The behaviour of the Vishniac instability during such a transition would be interesting to see. The instability is also likely to be limited by the presence of magnetic fields parallel to the shock front which act to limit the compression ratio of the shell and its bending through magnetic pressure and tension respectively.

Mac Low & Norman (1993) note that the Vishniac instability acts more strongly in SNRs than in WBBs because of the more rapid deceleration of SNRs. However, the deceleration of SNRs around and after the time of shell formation is complex (see, e.g., Bandiera & Petruk 2004). Furthermore, the window of opportunity during which the Vishniac instability can operate is much smaller in SNRs than in WBBs

because the continued energy injection in WBBs keeps the Mach number of the shell higher for longer (above the critical value of  $\sim 2.6$  for SNRs and  $\sim 3.6$  for WBBs). Thus the Vishniac instability might actually have a greater effect on the integrity of the cold shells around WBBs than those around SNRs.

Regardless of how the Vishniac instability creates ruptures, we find that it is the hotter interior gas which exists behind the cold shell of WBBs that ultimately allows blisters to develop to a larger relative size compared to those on SNRs. The hotter interior allows gas to vent through ruptures at substantially higher speed from WBBs than from SNRs, and so supplies a larger energy flux with which to grow a blister for a given size rupture (the latter is related to the thickness of the cold shell and ultimately to the shell radius). We note that this difference between WBB and SNR models may be mitigated somewhat in WBB models which adopt a lower wind speed, and/or by mass-loading of the bubble interior, either due to evaporation from the inside surface of the cold shell (Weaver et al. 1977), or due to the ablation or evaporation of embedded clumps (Pittard et al. 2001a,b).

Finally, we may wonder at the necessary conditions for the Vishniac instability to fragment/rupture a cold shell. It is currently unclear whether this occurs naturally once the perturbations become much thicker than the shell, or whether the blowout seen in Fig. 7 required the presence of the additional structure/perturbations in the flow. We intend to address this question in a future hydrodynamical investigation.

## ACKNOWLEDGEMENTS

JMP would like to thank the referee for a report which led to greater clarification of some parts of the paper. JMP gratefully acknowledges past funding from the Royal Society for a University Research Fellowship and current funding from the STFC. JMP would also like to thank Tom Hartquist for introducing him to the Meaburn et al. (1988) work on self-sealing bubbles while discussing shell ruptures and blowouts at a conference in Sexten, Italy, in July 2012.

## REFERENCES

- Bandiera R., Petruk O., 2004, *A&A*, 419, 419
- Blondin J.M., Marks B.S., 1996, *New Astr.*, 1, 235
- Blondin J.M., Wright E.B., Borkowski K.J., Reynolds S.P., 1998, *ApJ*, 500, 342
- Chevalier R.A., 1974, *ApJ*, 188, 501
- Chu Y.-H., Dickel J.R., Staveley-Smith L., Osterberg J., Smith R.C., 1995, *AJ*, 109, 4
- Comerón F., 1997, *A&A*, 326, 1195
- Danks A.C., Sembach K.R., 1995, *AJ*, 109, 2627
- Dwarkadas V.V., 2001, *JKAS*, 34, 243
- Dwarkadas V.V., 2007, *ApJ*, 667, 226
- Dyson J.E., Williams D.A., 1980, “The Physics of the Interstellar Medium”
- Edens A.D., Adams R.G., Rambo P., Ruggles L., Smith I.C., Porter J.L., Ditmire T., 2010, *Phys. Plasmas*, 17, 112104

- Falle S.A.E.G., 1981, MNRAS, 195, 1011
- Freyer T., Hensler G., Yorke H.W., 2006, ApJ, 638, 262
- García-Segura G., Langer N., Mac Low M.-M., 1996, A&A, 316, 133
- García-Segura G., Mac Low M.-M., 1995, ApJ, 455, 160
- Greidanus H., Strom R.G., 1992, A&A, 257, 265
- Gvaramadze V., 1998, Astr. Letters, 24, 144
- Gvaramadze V., 1999, A&A, 352, 712
- Harper-Clark E., Murray N., 2009, ApJ, 693, 1696
- Hester J.J., 1987, ApJ, 314, 187
- Jenkins E.B., Wallerstein G., Silk J., 1984, ApJ, 278, 649
- Krause M., Fierlinger K., Diehl R., Burkert A., Voss R., Ziegler U., 2013, A&A, 550, A49
- Liang E., Keilty K., 2000, ApJ, 533, 890
- Mac Low M.-M., McCray R., 1988, ApJ, 324, 776
- Mac Low M.-M., Norman M.L., 1993, 407, 207
- Mansfield V.N., Salpeter E.E., 1974, ApJ, 190, 305
- McKee C.F., Ostriker J.P., 1977, ApJ, 218, 148
- Meaburn J., Dyson J. E., Hartquist T. W., 1988, MNRAS, 230, 243
- Meaburn J., Whitehead M.J., Raymond J.C., Clayton C.A., Marston A.P., 1990, A&A, 227, 191
- Meaburn J., Wang L., Bryce M., 1995, A&A, 293, 532
- Meaburn J., Redman M.P., Boumis P., Harvey E., 2010, MNRAS, 408, 1249
- Michaut C., Cavet C., Bouquet S.E., Roy F., Nguyen H.C., 2012, ApJ, 759, 78
- Ntormousi E., Burkert A., Fierlinger K., Heitsch F., 2011, ApJ, 731, 13
- Pittard J.M., 2011, MNRAS, 411, L41
- Pittard J.M., Arthur S.J., Dyson J.E., Falle S.A.E.G., Hartquist T.W., Knight M.I., Pexton M., 2003, A&A, 401, 1027
- Pittard J.M., Dyson J.E., Hartquist T.W., 2001a, A&A, 367, 1000
- Pittard J.M., Hartquist T.W., Dyson J.E., 2001b, A&A, 373, 1043
- Redman M.P., Al-Mostafa Z.A., Meaburn J., Bryce M., Dyson J.E., 1999, A&A, 345, 943
- Rogers H., Pittard J. M., 2013, MNRAS, 431, 1337
- Ryu D., Vishniac E.T., 1987, ApJ, 313, 820
- Ryu D., Vishniac E.T., 1988, ApJ, 331, 350
- Sedov L.I., 1959, "Similarity and Dimensional Methods in Mechanics" (New York: Academic)
- Shull P.Jr., 1983, ApJ, 269, 218
- Strickland D.K., Stevens I.R., 1998, MNRAS, 297, 747
- Taylor G.I., 1950, Proc. R. Soc. London A, 201, 159
- Tenorio-Tagle G., Mñoz-Tuñón C., Pérez E., Silich S., Telles E., 2006, ApJ, 643, 186
- Toalá J.A., Arthur S.J., 2011, ApJ, 737, 100
- Tóth G., Draine B.T., 1993, ApJ, 413, 176
- van Marle A.J., Meliani Z., Marcowith A., 2012, A&A, 541, L8
- van Veelen B., Langer N., Vink J., García-Segura G., van Marle A.J., 2009, 503, 495
- Vishniac E.T., 1983, ApJ, 274, 152
- Vishniac E.T., 1994, ApJ, 428, 186
- Vishniac E.T., Ryu D., 1989, ApJ, 337, 917
- Wang L., 1992, ESO Messenger, 69, 34
- Weaver R., McCray R., Castor J., Shapiro P., Moore R., 1977, ApJ, 218, 377